

Discrete Time Crystals in Noninteracting Dissipative Systems

Gourab Das^{1,†} Saptarshi Saha^{2,‡} and Rangeet Bhattacharyya^{1,★}

¹*Department of Physical Sciences, Indian Institute of Science Education and Research Kolkata, Mohanpur 741246, India*

²*Institute for Physics and Astronomy (IFPA), Technische Universität Berlin, EW 7-1, Hardenbergstr. 36, 10623 Berlin, Germany*

Abstract

Many-body quantum systems, under suitable conditions, exhibit time-translation symmetry breaking and settle in a discrete time crystalline (DTC) phase – an out-of-equilibrium quantum phase of matter. The defining feature of DTC is a robust subharmonic response. However, the DTC phase is fragile in the presence of environmental dissipation. Here, we propose and exemplify a DTC phase in a noninteracting system that owes its stability to environmental dissipation. The lifetime of this DTC is independent of initial conditions and the size of the system, though it depends on the frequency of the external driver. We experimentally demonstrate this realization of DTC using Nuclear Magnetic Resonance spectroscopy.

INTRODUCTION

Discrete time crystals (DTC) were proposed in periodically driven quantum systems to exhibit discrete symmetry breaking in non-equilibrium systems [1–11]. Multiple groups experimentally realized the theoretical propositions over the last decade [6–15]. These works defined the DTC phase as, when a T -periodic drive, $H(t+T) = H(t)$, on a system produces a rigid reduced periodicity for a certain physical observable \hat{O} , i.e. $\langle \hat{O} \rangle(t+nT) = \langle \hat{O} \rangle(t)$ where n is an integer and $n \geq 2$. The key feature of DTC is its robustness against the errors in the drive, promising its potential as a stabilizer against butterfly effects and heating [16].

These recent theories employ non-ergodic many-body systems for resisting the thermalization [8–11]. The interactions among the particles provide the robustness of DTC. As such, a stable time-crystal has been shown to occur in the presence of the many-body localization (MBL) regime with strong spatial disorder [8, 9, 11, 14, 15, 17–19]. As well as DTCs have been engineered with the help of bosonic self-trapping [6, 20–25], gradient interaction [26], Stark gradient fields [27, 28], confinement in domain-wall [29], quantum scars [30–34], and Floquet integrability [16]. However, Choi *et al.* demonstrated that MBL is not necessary by an experiment on nitrogen-vacancy centers, where a time crystal (TC) formed regardless of the disorder in the strongly interacting regime [15]. This experimental breakthrough gave birth to a new kind of TCs, later named as *clean time crystals* (cTC) [16]. These cTCs exhibit integrability emerging through dynamics, unlike inheriting it from a static Hamiltonian, for the case of Floquet TCs [8–11].

These studies focus on the unitary dynamics in closed systems, but DTCs become fragile

in the presence of environmental dissipation [35–37]. However, environmental dissipation can be a blessing in disguise for the stability of a periodic observable, where the system releases excess energy pumped by a periodic drive, with disturbance, to its environment via dissipation channels [38–41]. These are called dissipative DTC and have been observed experimentally [42, 43]. In this context, we have shown that small interacting quantum systems can give rise to prethermal DTC, exploiting the emergence of a prethermal plateau during spin-locking [44]

In this work, we show that (i) non-interacting quantum systems connected to a local environment can exhibit a robust subharmonic response like a DTC phase, (ii) the dissipation channels play crucial roles in stabilizing the DTC. Specifically, we show that having a short decoherence time and a long relaxation time favors the formation of DTC in these systems. This phase is stabilized with only environmental dissipation, without requiring interaction among the system’s constituents, like space crystals forming in the noninteracting systems [20].

SYSTEM

We consider a single two-level system (TLS) having its local environment acting as a heat bath. This TLS may be a magnetic dipole with the Zeeman Hamiltonian $\mathcal{H}_o = \hbar\omega_o\sigma^z/2$. Hence, the evolution of the system can be described by the Lindblad master equation as follows [35],

$$\frac{d\rho}{dt} = -\frac{i}{\hbar} [\mathcal{H}_o, \rho] + \sum_{j=1}^3 \left(L_j \rho L_j^\dagger - \frac{1}{2} \{ L_j^\dagger L_j, \rho \} \right) \quad (1)$$

where, $L_1 = \sqrt{\frac{1+M_o}{2T_1}}\sigma^+$, $L_2 = \sqrt{\frac{1-M_o}{2T_1}}\sigma^-$, $L_3 = \sqrt{\frac{1}{2T_\phi}}\sigma^z$ and M_o is the magnetization of the system. Hence, in the interaction representation (with respect to \mathcal{H}_o), the magnetization follows the following Bloch equations [45],

$$\frac{dM_x}{dt} = -\frac{M_x}{T_2}, \quad \frac{dM_y}{dt} = -\frac{M_y}{T_2}, \quad \frac{dM_z}{dt} = \frac{M_o - M_z}{T_1} \quad (2)$$

where, $\frac{1}{T_2} = \frac{1}{2T_1} + \frac{1}{T_\phi}$. Here, T_1 represents the relaxation timescale, T_ϕ is the dephasing timescale, and T_2 is the decoherence timescale of the system, and they have standard representation. Let us suppose that the environment has a longer relaxation timescale compared to its decoherence timescale, i.e., $T_1 \gg T_2$.

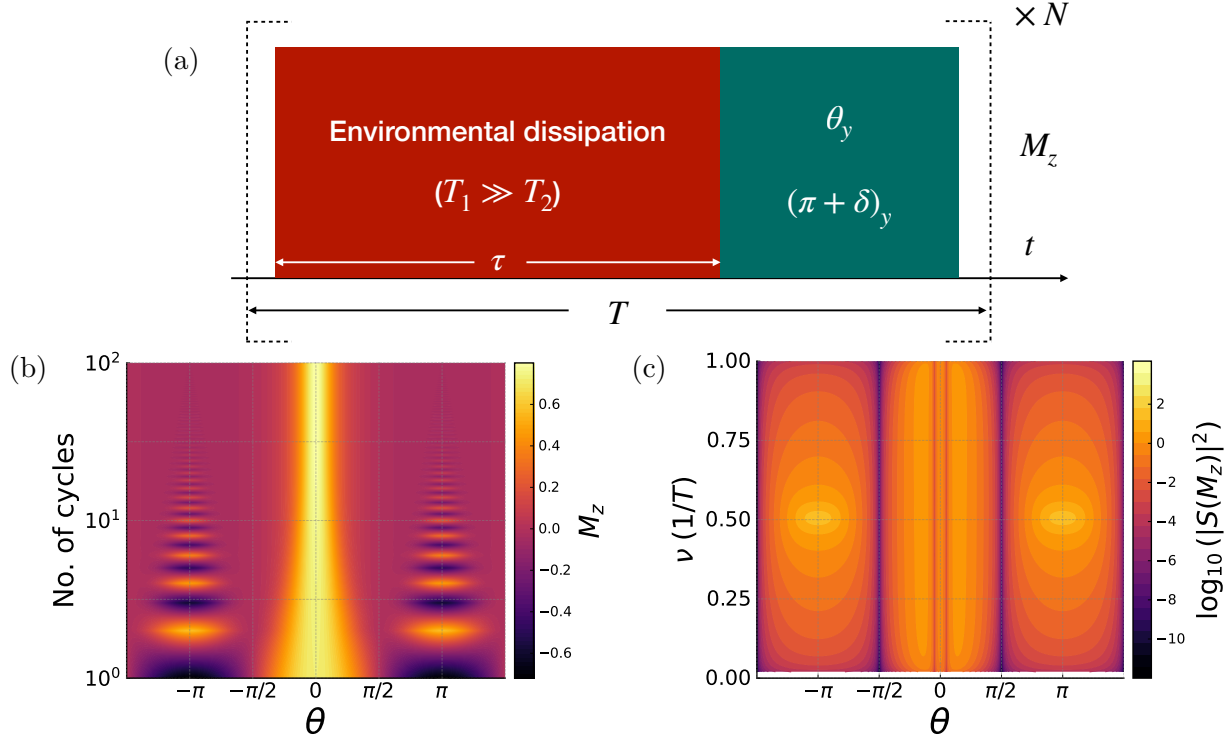


FIG. 1. (color online) (a) Pulse sequence for environment-assisted DTC. Here, the system interacts with its environment for a τ time period (red, deeper grey) and is followed by a θ -pulse about y -direction (green, lighter grey), and this sequence, having T periodicity, is repeated many times. As $T_1 \gg T_2$, relaxation of M_z is slower than the decay of M_x . Hence, the time delay τ acts similarly to a spin-locking pulse along z -direction [15, 46]. Whilst, the θ -pulse, when close to π , provides the $2T$ -periodicity for M_z . (b) The existence of DTC depends on the θ -pulse. Here M_z oscillates between positive and negative values in alternate cycles when θ is close to $\pm\pi$. (c) Spectrum of M_z in the frequency domain. The Fourier spectrum shows peaks around $\nu = 0.5$ frequency, confirming the $2T$ -periodicity of M_z in the same regions of θ . The parameters used to generate the plots of (b) and (c) are $T_1 = 100T_2$, $\tau = 10T_2$, $M_0 = 0.8$, and $M_z(0) = -0.9M_0$.

Next, a $\theta = \pi + \delta$ rotation is applied about the y -direction, as shown in Fig. 1. The corresponding Hamiltonian, in the interaction picture of \mathcal{H}_0 , is $H_y = \hbar\omega_1\sigma^y/2$, where $\omega_1(T - \tau) = \pi + \delta$. Usually, a strong pulse is provided for the θ -rotation to keep the pulse duration small, hence the dissipation during the excitation pulse is ignored [46]. The corresponding

dynamics is governed by the von Neumann-Liouville equation, as follows [35],

$$\frac{d\rho}{dt} = -\frac{i}{\hbar} [H_y, \rho] \quad \text{for } \tau < t \leq T \quad (3)$$

To obtain $2T$ -periodicity the mentioned sequence, in Fig. 1(a), is repeated N times ($N \in \mathcal{I}$). Hence, the final density matrix, in the Liouville space, after N -cycle can be written as,

$$\hat{\rho}(NT) = \left[e^{\hat{\mathcal{L}}_y(T-\tau)} e^{\hat{\mathcal{L}}_\tau \tau} \right]^N \hat{\rho}(0) \quad (4)$$

Here, $\hat{\mathcal{L}}_y$ is the Liouvillian refers to the rotation about y direction, from Eq. 3, and $\hat{\mathcal{L}}_\tau$ is the same corresponding to system's interaction with its environment during the τ -time delay, from Eq. 2.

EMERGENCE OF THE DTC PHASE

The system's dynamics can be tracked easily in the parts of the pulse sequence in Fig. 1(a). During the time delay τ , the system follows the Bloch equations [45], as given in Eq. 2. For the initial magnetization $\mathbf{M} = (M_x^0, M_y^0, M_z^0)$, the solutions are,

$$\begin{aligned} M_x(t) &= M_x^0 e^{-\frac{t}{T_2}} \equiv M_x^\tau(M_x^0, t) \\ M_y(t) &= M_y^0 e^{-\frac{t}{T_2}} \equiv M_y^\tau(M_y^0, t) \\ M_z(t) &= M_\circ \left(1 - e^{-\frac{t}{T_1}} \right) + M_z^0 e^{-\frac{t}{T_1}} \equiv M_z^\tau(M_z^0, t) \end{aligned} \quad (5)$$

Therefore, after the τ time delay $M_{x/y}^\tau(M_{x/y}^0, \tau) \approx 0$ and $M_z^\tau(M_z^0, \tau) \approx M_z^0$, if $T_2 < \tau \ll T_1$. Hence, M_z relaxes slower than the decay of other magnetization components; in turn, a time delay of τ , with this timescale separation, acts similarly to the spin-locking pulse along the z -direction [15, 44, 46–48], i.e. required for the rigidity of DTC phase [16]. Therefore, we can use a pulse sequence, similar to Beatrez *et al.* [46], where the system interacts with the environment for τ time duration, instead of the spin-locking pulse, as shown in Fig. 1(a).

As the θ rotation around the y -direction occurs for a short duration, the dissipation can be neglected during this period. Therefore, the dynamics are adequately described by the first-order process.

Solution for $\theta = \pi$

For a perfect π pulse, with initial condition $\mathbf{M} = (0, 0, M_z^0)$ we get (see Appendix A for more details),

$$\begin{aligned} M_z(T) &= -M_z^\tau(M_z^0, \tau) \\ M_z(2T) &= -M_z^\tau(-M_z^\tau(M_z^0, \tau), \tau) \end{aligned} \quad (6)$$

Here, all other magnetization components vanish. As $\tau \ll T_1$, M_z reverses its sign after time T , returning near the initial value after $2T$ time, i.e., after the second π -pulse. Hence, the perfect π pulse provides $2T$ -periodicity producing DTC phase. However, the DTC vanishes in the timescale of T_1 , as M_z relaxes with T_1 timescale. As the system consists of noninteracting particles, the lifetime of this DTC phase is independent of particle numbers, unlike previously reported DTCs [16].

Solution for $\theta = \pi + \delta$ with $\delta/\pi \rightarrow 0$

Here, we check the rigidity of DTC phase by applying a perturbation (δ) in the π rotation, i.e. $\theta = \pi + \delta$, and we get,

$$\begin{aligned} M_x(T) &= -M_z^\tau(M_z^0, \tau) \delta; \quad M_x(2T) = -M_x^\tau(-M_z^\tau(M_z^0, \tau) \delta, \tau) - M_z^\tau(-M_z^\tau(M_z^0, \tau), \tau) \delta \\ M_z(T) &= -M_z^\tau(M_z^0, \tau); \quad M_z(2T) = -M_z^\tau(-M_z^\tau(M_z^0, \tau), \tau) + M_x^\tau(-M_z^\tau(M_z^0, \tau) \delta, \tau) \delta \end{aligned} \quad (7)$$

Here, the period doubling of M_z is absent in the Eq. 7 due to the M_x^τ term. DTC phase can be retrieved if $\delta \rightarrow 0$ or $T_2 < \tau$. However, we need that $\tau \ll T_1$, otherwise M_z will relax back near to M_0 preventing the existence of DTC, as shown in Fig. 2 and 3(a,b). The lifetime, which is inversely proportional to the full width at half maximum (FWHM) of M_z in the frequency domain [44], of DTC phase vanishes as δ^2 due to the error term in M_z varies at the same rate (Eq. 7), as shown in Fig. 3(c). We name this environment-assisted DTC as EDTC.

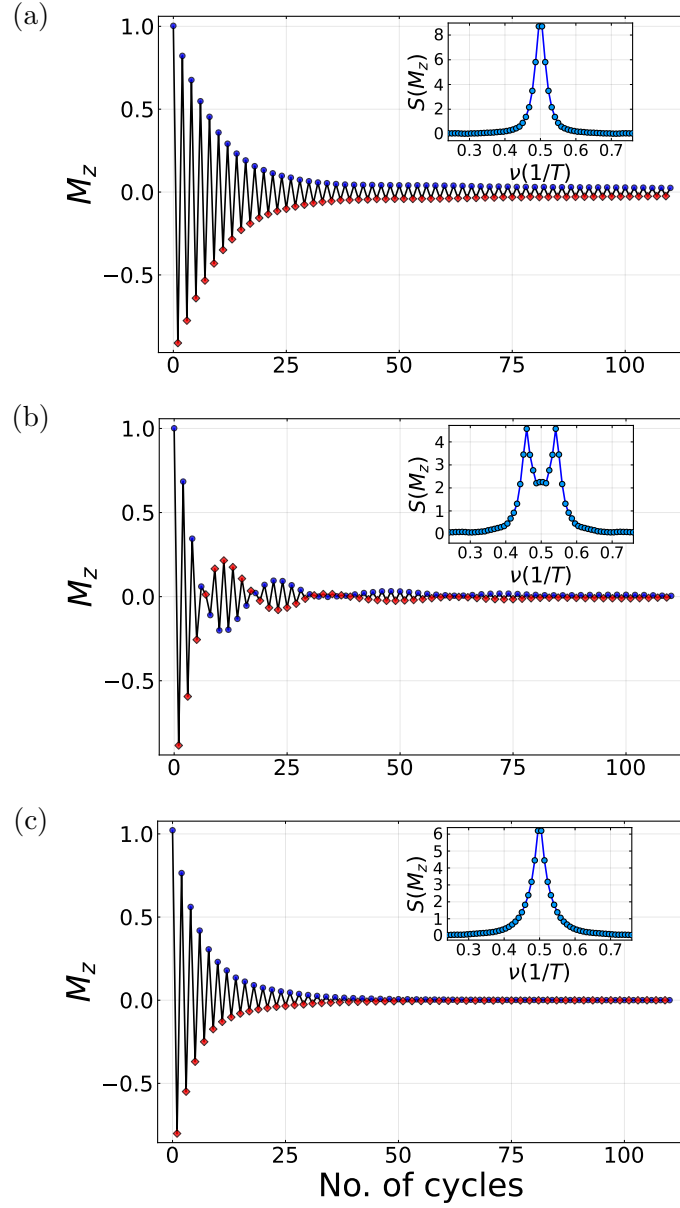


FIG. 2. (color online) Plots of experimentally determined values of M_z versus the number of cycles are shown in (a), (b), (c) and their corresponding Fourier transform, $S(M_z)$, versus frequency (ν) are shown in the insets. (a) Perfectly calibrated π pulses are used to get the DTC phase, which produces a sharp peak at 0.5 in the frequency domain. Here $\tau = 25ms$. (b) In this case the pulses were with error of $\delta = 0.0674\pi$, with $\tau = 25ms$, kills the DTC phase to produce a decaying beat pattern. This corresponds to peaks at $0.5(1 \pm \delta)$ in the frequency domain. (c) Here, the time delay has been increased, $\tau = 0.2s$, for the same imperfect pulse of (b) to get back DTC, showing the rigidity of such a phase. However, the lifetime of DTC has reduced significantly.

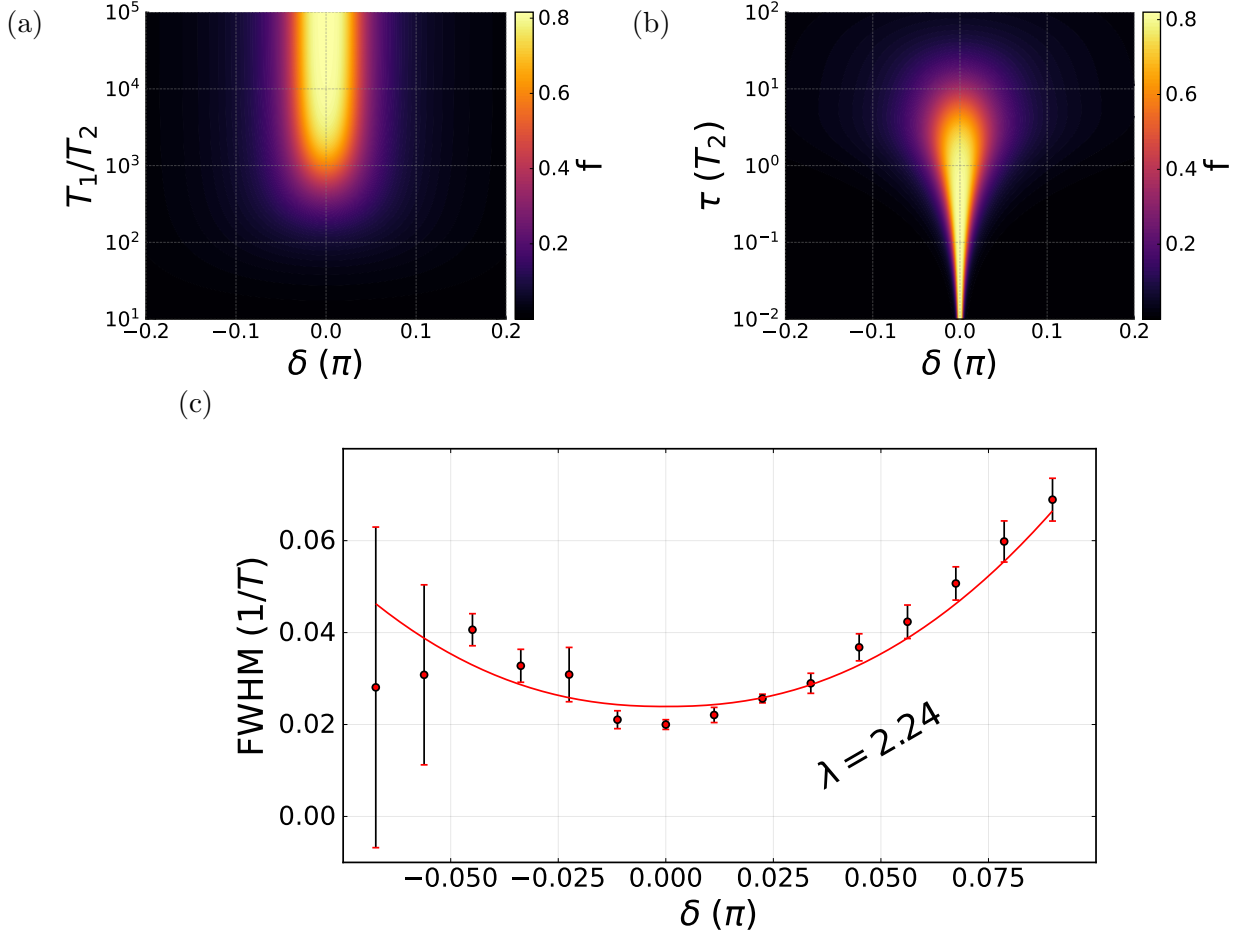


FIG. 3. (color online) (a) Crystalline fraction (f), defined by Choi *et al.* [15], dependence on the perturbation (δ) in the π rotation about y -direction and the ratio of the timescales T_1 and T_2 . The Crystalline fraction, f , acts as a measure for the amount of DTC phase present in the system. To have DTC phase δ needs to be small, i.e. we need near perfect π pulses and $T_2 \ll T_1$, as it follows from Eq. 7. We have used $\tau = 5T_2$ for the plot. (b) Crystalline fraction's dependence on δ and time interval τ (in the units of T_2). It shows δ needs to be small and $T_2 < \tau \ll T_1$ for having DTC phase, following Eq. 7. Here, $T_1 = 1000T_2$ is considered for the plot. The other parameters used to generate the plots, of (a) and (b), are $M_o = 0.8$, and $M_z(0) = -0.9M_o$. (c) Plot of the FWHM of the Fourier spectrum of M_z , i.e. $S(M_z)$, versus the error (δ) in π pulse (experimental data for $\tau = 25ms$). The data is fitted with $f(\delta) = a\delta^\lambda + b$ for $\lambda = 2.24$. Hence, FWHM varies as δ^2 ; therefore, the lifetime of the DTC phase decreases at the same rate.

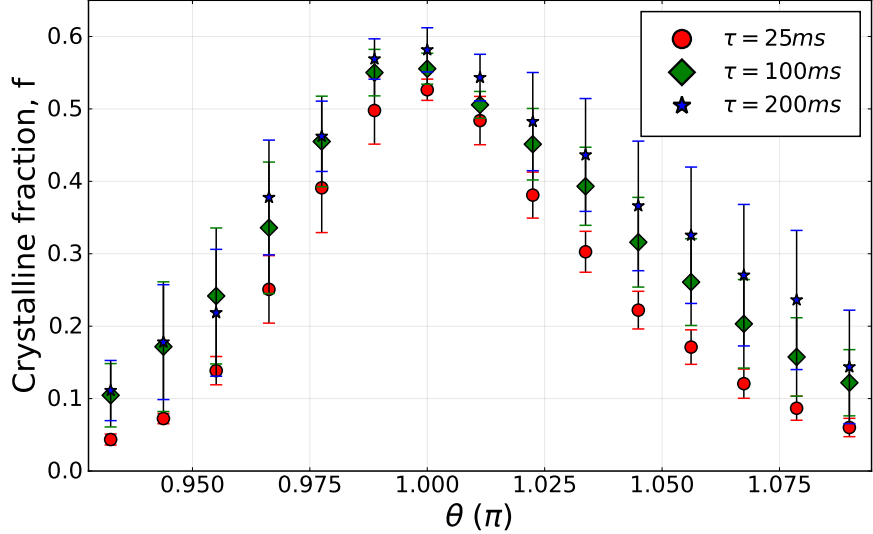


FIG. 4. (color online) The variation of Crystalline fraction, f , with θ pulse is plotted, with different time delays τ . It shows that we need a pulse very close to π , for a short τ , to get the EDTC phase. Whilst EDTC persists for imperfect pulses when a longer τ is applied, showing the rigidity of the phase.

EXPERIMENT

We use Nuclear Magnetic Resonance, an ensemble spectroscopy, to experimentally demonstrate our proposed scheme of realizing EDTC. As the sample, we use 99.9% D_2O , which is effectively a collection of HDO molecules to show the existence of such a phase. The nucleus of the Hydrogen atom, a lone proton, in the HDO molecule, serves as the spin-1/2 particle. We used a Bruker Avance III 500 MHz spectrometer to perform all the experiments, and the ambient temperature during the measurements was 25°C. We determined the relaxation times of protons in HDO as $T_1 \simeq 7.57s$, $T_2^* \sim 0.6s$. We used a uniform 16.7 kHz RF drive amplitude to apply various pulses in all the experiments. The variation of crystalline fraction, f , with respect to the θ pulse along the y -direction for three sets of time delay, τ (25ms, 100ms, 200ms), is shown in Fig. 4. It shows that we need near perfect π pulse to have an EDTC phase, however a longer τ can mitigate higher errors, δ , to preserve EDTC, thus validating the rigidity of such a phase.

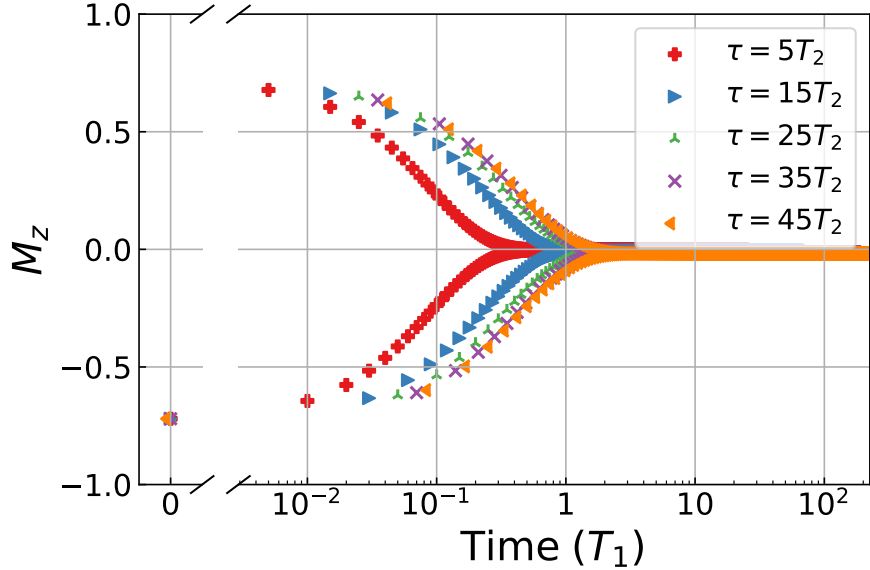


FIG. 5. (color online) The variation of M_z with time (in the units of T_1) is shown for different time delays τ 's. This shows the lifetime of this DTC increases with τ . Hence, the lifetime decreases with increasing frequency of the pulse. The parameters used to generate the plot are $T_1 = 1000T_2$, $\delta = 0.1\pi$, $M_z(0) = -0.9M_0$, and $M_0 = 0.8$.

DISCUSSION

We note the scheme relies on isolated TLS with its environment. As such, the experiment does not depend on the number of TLS chosen as long as the number is thermodynamically large. The FWHM of $S(M_z)$ does not depend on the initial magnetization, which is related to the initial state's temperature via the Boltzmann distribution. As such, the lifetime of the EDTC, like Floquet DTC phase, does not depend on the initial condition [8–11, 14, 49]. However, Fig. 5 show that it depends on the time delay τ , which is inversely proportional to the frequency of the θ pulse, when an erroneous pulse is provided, i.e., a property of prethermal TCs, though the lifetime is independent of the frequency in case of perfect pulses, as the dynamics is only governed by T_1 and T_2 dynamics [44, 50]. Hence, the EDTC phase is not a Floquet or prethermal DTC. We note the decoherence dissipator governs the system's dynamics during the time delay, τ . Hence, unlike the other DTCs, the EDTC phase lacks the Hamiltonian description and instead has a Liouvillian description.

CONCLUSIONS

To conclude, we show that the DTC phase, if defined through robust subharmonic response of a quantum system, having many-body interactions is not a strict necessity; the environment can provide robustness to dissipative systems. This is in line with our previous work demonstrating that a prethermal plateau can emerge in small dissipative systems too [44]. We show that an open quantum system, with the decoherence timescale much shorter compared to that of the relaxation ($T_2 \ll T_1$), can be manipulated to have an environment-assisted DTC phase. In fact, this EDTC phase does not require interactions among the system's constituents; hence, the lifetime of such a phase is independent of system size. This novel phase is neither a Floquet nor a prethermal DTC; also, it lacks a Hamiltonian description as a dissipator governs the dynamics during the τ -delay. We demonstrate the existence of such an EDTC phase using nuclear magnetic resonance spectroscopy.

Acknowledgments - GD gratefully acknowledges the Council of Scientific & Industrial Research (CSIR), India, for a research fellowship (File no: 09/921(0327)/2020-EMR-I). The authors thank Arpan Chatterjee, Sarfraz Fency, Shubhamay Panja, and Arkadeep Mitra for their insightful comments.

[†]gd20rs094@iiserkol.ac.in

[‡]s.saha@tu-berlin.de

^{*}rangeet@iiserkol.ac.in

- [1] Alfred Shapere and Frank Wilczek. Classical time crystals. *Phys. Rev. Lett.*, 109:160402, Oct 2012.
- [2] Frank Wilczek. Quantum time crystals. *Phys. Rev. Lett.*, 109:160401, Oct 2012.
- [3] Frank Wilczek. Superfluidity and space-time translation symmetry breaking. *Phys. Rev. Lett.*, 111:250402, Dec 2013.
- [4] Patrick Bruno. Comment on “quantum time crystals”. *Phys. Rev. Lett.*, 110:118901, Mar 2013.
- [5] Haruki Watanabe and Masaki Oshikawa. Absence of quantum time crystals. *Phys. Rev. Lett.*, 114:251603, Jun 2015.

- [6] Krzysztof Sacha. Modeling spontaneous breaking of time-translation symmetry. *Phys. Rev. A*, 91:033617, Mar 2015.
- [7] Anushya Chandran and S. L. Sondhi. Interaction-stabilized steady states in the driven $o(n)$ model. *Phys. Rev. B*, 93:174305, May 2016.
- [8] Vedika Khemani, Achilleas Lazarides, Roderich Moessner, and S. L. Sondhi. Phase structure of driven quantum systems. *Phys. Rev. Lett.*, 116:250401, Jun 2016.
- [9] Dominic V. Else, Bela Bauer, and Chetan Nayak. Floquet time crystals. *Phys. Rev. Lett.*, 117:090402, Aug 2016.
- [10] C. W. von Keyserlingk, Vedika Khemani, and S. L. Sondhi. Absolute stability and spatiotemporal long-range order in floquet systems. *Phys. Rev. B*, 94:085112, Aug 2016.
- [11] N. Y. Yao, A. C. Potter, I.-D. Potirniche, and A. Vishwanath. Discrete time crystals: Rigidity, criticality, and realizations. *Phys. Rev. Lett.*, 118:030401, Jan 2017.
- [12] Dominic V. Else, Bela Bauer, and Chetan Nayak. Prethermal phases of matter protected by time-translation symmetry. *Phys. Rev. X*, 7:011026, Mar 2017.
- [13] Vedika Khemani, C. W. von Keyserlingk, and S. L. Sondhi. Defining time crystals via representation theory. *Phys. Rev. B*, 96:115127, Sep 2017.
- [14] Jiehang Zhang, Paul W Hess, A Kyprianidis, Petra Becker, A Lee, J Smith, Gaetano Pagano, I-D Potirniche, Andrew C Potter, Ashvin Vishwanath, et al. Observation of a discrete time crystal. *Nature*, 543(7644):217–220, 2017.
- [15] Soonwon Choi, Joonhee Choi, Renate Landig, Georg Kucska, Hengyun Zhou, Junichi Isoya, Fedor Jelezko, Shinobu Onoda, Hitoshi Sumiya, Vedika Khemani, et al. Observation of discrete time-crystalline order in a disordered dipolar many-body system. *Nature*, 543(7644):221–225, 2017.
- [16] Biao Huang, Ying-Hai Wu, and W. Vincent Liu. Clean floquet time crystals: Models and realizations in cold atoms. *Phys. Rev. Lett.*, 120:110603, Mar 2018.
- [17] Dominic V Else, Christopher Monroe, Chetan Nayak, and Norman Y Yao. Discrete time crystals. *Annual Review of Condensed Matter Physics*, 11(1):467–499, 2020.
- [18] Vedika Khemani, Roderich Moessner, and SL Sondhi. A brief history of time crystals. *arXiv preprint arXiv:1910.10745*, 2019.
- [19] Fernando Iemini, Rosario Fazio, and Anna Sanpera. Floquet time crystals as quantum sensors of ac fields. *Phys. Rev. A*, 109:L050203, May 2024.

[20] Krzysztof Sacha. *Time crystals*, volume 114 of *Springer Series on Atomic, Optical, and Plasma Physics*. Springer, Cham, 2020.

[21] Sebastian Wüster, Beata J. Da browska Wüster, and Matthew J. Davis. Macroscopic quantum self-trapping in dynamical tunneling. *Phys. Rev. Lett.*, 109:080401, Aug 2012.

[22] Angelo Russomanno, Fernando Iemini, Marcello Dalmonte, and Rosario Fazio. Floquet time crystal in the lipkin-meshkov-glick model. *Phys. Rev. B*, 95:214307, Jun 2017.

[23] Krzysztof Giergiel, Arkadiusz Kuroś, and Krzysztof Sacha. Discrete time quasicrystals. *Phys. Rev. B*, 99:220303, Jun 2019.

[24] Paweł Matus and Krzysztof Sacha. Fractional time crystals. *Phys. Rev. A*, 99:033626, Mar 2019.

[25] Andrea Pizzi, Johannes Knolle, and Andreas Nunnenkamp. Higher-order and fractional discrete time crystals in clean long-range interacting systems. *Nature communications*, 12(1):2341, 2021.

[26] Rozhin Yousefjani, Angelo Carollo, Krzysztof Sacha, Saif Al-Kuwari, and Abolfazl Bayat. Non-hermitian discrete time crystals. *Phys. Rev. B*, 111:165117, Apr 2025.

[27] Shuo Liu, Shi-Xin Zhang, Chang-Yu Hsieh, Shengyu Zhang, and Hong Yao. Discrete time crystal enabled by stark many-body localization. *Phys. Rev. Lett.*, 130:120403, Mar 2023.

[28] A. Kshetrimayum, J. Eisert, and D. M. Kennes. Stark time crystals: Symmetry breaking in space and time. *Phys. Rev. B*, 102:195116, Nov 2020.

[29] Mario Collura, Andrea De Luca, Davide Rossini, and Alessio Lerose. Discrete time-crystalline response stabilized by domain-wall confinement. *Phys. Rev. X*, 12:031037, Sep 2022.

[30] N. Maskara, A. A. Michailidis, W. W. Ho, D. Bluvstein, S. Choi, M. D. Lukin, and M. Serbyn. Discrete time-crystalline order enabled by quantum many-body scars: Entanglement steering via periodic driving. *Phys. Rev. Lett.*, 127:090602, Aug 2021.

[31] Wentai Deng and Zhi-Cheng Yang. Using models with static quantum many-body scars to generate time-crystalline behavior under periodic driving. *Phys. Rev. B*, 108:205129, Nov 2023.

[32] Kieran Bull, Andrew Hallam, Zlatko Papić, and Ivar Martin. Tuning between continuous time crystals and many-body scars in long-range xyz spin chains. *Phys. Rev. Lett.*, 129:140602, Sep 2022.

[33] Biao Huang, Tsz-Him Leung, Dan M. Stamper-Kurn, and W. Vincent Liu. Discrete time

crystals enforced by floquet-bloch scars. *Phys. Rev. Lett.*, 129:133001, Sep 2022.

[34] Biao Huang. Analytical theory of cat scars with discrete time-crystalline dynamics in floquet systems. *Phys. Rev. B*, 108:104309, Sep 2023.

[35] Heinz-Peter Breuer and Francesco Petruccione. *The theory of open quantum systems*. Oxford University Press, 2002.

[36] Achilleas Lazarides and Roderich Moessner. Fate of a discrete time crystal in an open system. *Phys. Rev. B*, 95:195135, May 2017.

[37] Andreu Riera-Campeny, Maria Moreno-Cardoner, and Anna Sanpera. Time crystallinity in open quantum systems. *Quantum*, 4:270, 2020.

[38] Rozhin Yousefjani, Angelo Carollo, Krzysztof Sacha, Saif Al-Kuwari, and Abolfazl Bayat. Non-hermitian discrete time crystals. *arXiv preprint arXiv:2410.22713*, 2024.

[39] Zongping Gong, Yuto Ashida, Kohei Kawabata, Kazuaki Takasan, Sho Higashikawa, and Masahito Ueda. Topological phases of non-hermitian systems. *Phys. Rev. X*, 8:031079, Sep 2018.

[40] F. M. Gambetta, F. Carollo, M. Marcuzzi, J. P. Garrahan, and I. Lesanovsky. Discrete time crystals in the absence of manifest symmetries or disorder in open quantum systems. *Phys. Rev. Lett.*, 122:015701, Jan 2019.

[41] Achilleas Lazarides, Sthitadhi Roy, Francesco Piazza, and Roderich Moessner. Time crystallinity in dissipative floquet systems. *Phys. Rev. Res.*, 2:022002, Apr 2020.

[42] Hans Keßler, Phatthamon Kongkhambut, Christoph Georges, Ludwig Mathey, Jayson G. Cosme, and Andreas Hemmerich. Observation of a dissipative time crystal. *Phys. Rev. Lett.*, 127:043602, Jul 2021.

[43] Hossein Taheri, Andrey B Matsko, Lute Maleki, and Krzysztof Sacha. All-optical dissipative discrete time crystals. *Nature communications*, 13(1):848, 2022.

[44] Saptarshi Saha and Rangeet Bhattacharyya. Prethermal discrete time crystal in driven-dissipative dipolar systems. *Phys. Rev. A*, 109:012208, Jan 2024.

[45] F. Bloch. Nuclear induction. *Phys. Rev.*, 70:460–474, Oct 1946.

[46] William Beatrez, Christoph Fleckenstein, Arjun Pillai, Erica de Leon Sanchez, Amala Akkiraju, Jesus Diaz Alcala, Sophie Conti, Paul Reshetikhin, Emanuel Druga, Marin Bukov, et al. Critical prethermal discrete time crystal created by two-frequency driving. *Nature Physics*, 19(3):407–413, 2023.

[47] Saptarshi Saha and Rangeet Bhattacharyya. Cascaded dynamics of a periodically driven dissipative dipolar system. *Physical Review A*, 107(2):022206, 2023.

[48] Arnab Chakrabarti and Rangeet Bhattacharyya. Emergence of prethermal states in a driven dissipative system through cross-correlated dissipation. *Europhysics Letters*, 142(5):55001, 2023.

[49] C. W. von Keyserlingk and S. L. Sondhi. Phase structure of one-dimensional interacting floquet systems. ii. symmetry-broken phases. *Phys. Rev. B*, 93:245146, Jun 2016.

[50] Francisco Machado, Dominic V. Else, Gregory D. Kahanamoku-Meyer, Chetan Nayak, and Norman Y. Yao. Long-range prethermal phases of nonequilibrium matter. *Phys. Rev. X*, 10:011043, Feb 2020.

Appendix A: Dynamics to the DTC phase

As the θ rotation around y -direction occurs for a short duration, the dissipation can be neglected during this period. Therefore, the dynamics are adequately described by the first-order process, with the initial magnetization $\mathbf{M} = (m_x^0, m_y^0, m_z^0)$ the solution for Eq. 3 is given as,

$$\begin{aligned} M_x(t) &= m_x^0 \cos \theta + m_z^0 \sin \theta \equiv M_x^{\text{rot}}(m_x^0, m_z^0, \theta) \\ M_y(t) &= m_y^0 \equiv M_y^{\text{rot}}(m_y^0, \theta) \\ M_z(t) &= m_z^0 \cos \theta - m_x^0 \sin \theta \equiv M_z^{\text{rot}}(m_x^0, m_z^0, \theta) \end{aligned} \quad (\text{A1})$$

Therefore, $M_x^{\text{rot}}(m_x^0, m_z^0, \theta) \approx -m_x^0$, $M_y^{\text{rot}}(m_y^0, \theta) = m_y^0$, and $M_z^{\text{rot}}(m_x^0, m_z^0, \theta) \approx -m_z^0$ after the θ -pulse for $\theta \approx \pm\pi$.

To study the emergence of the DTC phase, we provide the analytical solution of $M_z(t)$ up to $2T$ time period by solving Eq. 4. For initial condition $\mathbf{M} = (0, 0, M_z^0)$, the magnetization at time τ is given as,

$$M_x(\tau) = 0; \quad M_z(\tau) = M_z^\tau(M_z^0, \tau) \quad (\text{A2})$$

After the θ rotation about y -direction, the magnetization is given by,

$$M_x(T) = M_z^\tau(M_z^0, \tau) \sin \theta; \quad M_z(T) = M_z^\tau(M_z^0, \tau) \cos \theta \quad (\text{A3})$$

Similarly, after a time $T + \tau$, the magnetization is,

$$\begin{aligned} M_x(T + \tau) &= M_x^\tau(M_z^\tau(M_z^0, \tau) \sin \theta, \tau) \\ M_z(T + \tau) &= M_z^\tau(M_z^\tau(M_z^0, \tau) \cos \theta, \tau) \end{aligned} \quad (\text{A4})$$

Finally, after the $2T$ time, the magnetization becomes,

$$\begin{aligned} M_x(2T) &= M_x^\tau(M_z^\tau(M_z^0, \tau) \sin \theta, \tau) \cos \theta + M_z^\tau(M_z^\tau(M_z^0, \tau) \cos \theta, \tau) \sin \theta \\ M_z(2T) &= M_z^\tau(M_z^\tau(M_z^0, \tau) \cos \theta, \tau) \cos \theta - M_x^\tau(M_z^\tau(M_z^0, \tau) \sin \theta, \tau) \sin \theta \end{aligned} \quad (\text{A5})$$

Here, M_y does not evolve, as y is the symmetry axis.